Macromolecules
ARTICLE

Macromolecules **2010**, *43*, 9257–9267 **9257**
DOI: 10.1021/ma101979p

Thermodynamic Properties of Copper Complexes Used as Catalysts in Atom Transfer Radical Polymerization

Nicola Bortolamei,[†] Abdirisak A. Isse,[†] Valerio B. Di Marco,[†] Armando Gennaro,*[,†] and Krzysztof Matyjaszewski[‡]

[†]*Department of Chemical Sciences, University of Padova, via Marzolo 1, 35131 Padova, Italy, and* [‡]*Department of Chemistry, Carnegie Mellon University, 4400 Fifth Avenue, Pittsburgh, Pennsylvania 15213, United States*

Received August 26, 2010; Revised Manuscript Received October 7, 2010

ABSTRACT: The thermodynamic properties of some copper complexes, among those frequently used as catalysts in controlled/living radical polymerization, has been studied in CH_3CN + 0.1 M $(C_2H_5)_4NBF_4$. A combination of different techniques, namely potentiometry, spectrophotometry and cyclic voltammetry, has been used to determine the stability constants of all possible complexes of Cu^I and Cu^{II} present in binary and ternary systems composed of Cu^I or Cu^{II}, a halide ion ($X = Cl^-$, Br^-) and a polyamine ligand (L = pentamethyldiethylenetriamine, tris(2-dimethylaminoethyl)amine). The binary Cu−X systems show only mononuclear CuX_x complexes, where $x = 1, 2, 3, 4$ for Cu^{II}, and $x = 1, 2$ for Cu^I. Conversely, in the case of the binary Cu−L systems, besides the mononuclear complexes CuL_l, where $l = 1$ or 2, also dinuclear complexes Cu_2L were found. The ternary systems give rise to a mixture of mononuclear and dinuclear complexes of general formula $Cu_mL_lX_x$. Besides the 1:1:1 complex obtained in all combinations, the following species were found: $Cu^{II}LX_2$, $Cu^I{}_2LX$ and $Cu^I{}_2LX_2$. The stability constants of all these species were determined and used to construct speciation diagrams for both Cu^I and Cu^{II} species. Such diagrams show that often conditions favoring the quantitative formation of $Cu^{II}L$, $Cu^{II}L_2$, or $Cu^{II}LX$ can be easily realized, whereas isolation of a single predominant Cu^I species can hardly be achieved. Speciation diagrams for Cu^I as a function of C_X/C_{Cu^I} show interesting results that may be helpful in rationalizing the role of termination reactions in atom transfer radical polymerization.

Introduction

Controlled or living radical polymerization is a powerful process, which allows the preparation of (co)polymers with well-defined features such as high molecular weights, narrow molecular weight distributions ($M_w/M_n < 1.1$), and precise molecular architectures.[1] Since its discovery about a decade ago,[2,3] the metal catalyzed controlled/living radical polymerization has attracted much attention and has witnessed explosive growth and development.[4,5] It is based on a reversible halogen atom transfer between a dormant macromolecular species (P_m−X) and a low oxidation state metal complex (Scheme 1), resulting in the formation of propagating radicals ($P_m^•$) and the metal complex in a higher oxidation state. Thus, the process was coined atom transfer radical polymerization (ATRP),[2] which is among the most widely used controlled radical polymerization techniques.[6]

The precise mechanism of this reaction is still under investigation. In particular, three possible mechanisms, namely halogen atom transfer, outer-sphere electron transfer (ET) and concerted dissociative ET, have been considered for the activation step.[7] The success of ATRP relies strongly on the equilibrium between the activation step in which the propagating radicals are generated and the deactivation step in which the latter are converted to dormant species. This equilibrium is strongly shifted toward the dormant species ($K_{ATRP} < 10^{-4}$)[8] and, hence, the rate of bimolecular radical termination is drastically diminished.

Although several transition metals have shown catalytic properties toward various organic halides used as initiators,[9,10] copper complexes with nitrogen ligands are the most used catalysts thanks to their low cost and easy handling; typically, they are prepared *in situ* by adding the ligand to a cuprous halide salt. One limitation of early ATRP was the large amount of catalyst used, which leads to polymers with a significant amount of residual metals due to the progressive accumulation of the deactivating complex $X-Mt^{z+1}L_l$ because of the bimolecular termination reaction.[6] To overcome this problem, several strategies for regenerating the catalyst by reduction have been developed.[11−15]

Despite the fundamental role played by Cu complexes utilized as catalysts in ATRP, relatively little attention has been devoted to the identification of the species really present in the reaction medium. Studies on the catalytic system are crucial not only for understanding the reaction mechanism but also for further developments of ATRP as well as its industrial applications. Indeed, both the kinetics of activation of initiators by copper complexes and ATRP equilibrium have been widely investigated,[16−18] with particular attention to the construction of valuable correlations between catalytic activity and several properties of the complexes, including molecular structure,[19−21] redox potentials,[22−24] or ligand/metal ratio and nature of counterion.[25,26]

However, due to the paucity of data on the stability constants of copper complexes in organic media,[27,28] the possibility that complex equilibria may play an important role in the reaction mechanism has not been considered yet. Indeed, the precise nature of the activator copper complex has never been clarified; many papers on ATRP refer to the Cu^I catalyst as Cu^IX/L, which simply indicates the composition of the mixture for the *in situ* preparation of the catalyst rather than its stoichiometry and structure. Detailed analysis of the speciation of copper under the usual ATRP conditions is highly desired to appropriately address

*Corresponding author. E-mail: armando.gennaro@unipd.it.

Published on Web 10/22/2010

Scheme 1

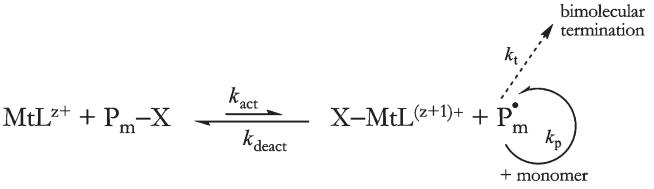

Scheme 2. Chemical Structures of Investigated Ligands and Some Schematic Representations of the Molecular Geometry of Cu Complexes

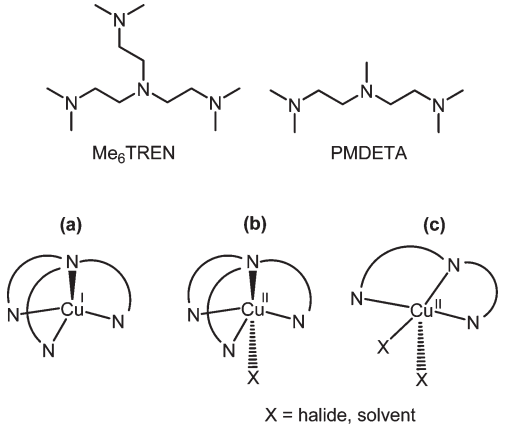

this fundamental aspect of the process. In fact, it has been shown that the catalytic activity strongly depends on the relative stabilization of the two copper oxidation states as well as their relative affinities for the halide ions.[10,28,29]

Moreover, recent developments in the field of copper-catalyzed ATRP, such as activator regenerated by electron transfer (ARGET)[30−33] ATRP, make use of metallic Cu both as activator and precursor of the active Cu^I complex. Metallic Cu formed by disproportionation of Cu^I was also proposed to play a crucial role in the so-called single electron transfer living radical polymerization (SET−LRP)[34−36] in which the carbon−halogen bond in the dormant species is thought to be exclusively activated by Cu^0. Knowledge of the relative stabilities of Cu^I and Cu^{II} complexes, allowing full assessment of the comproportionation (or disproportionation) equilibria, will be of great help for the comprehension of the activation mechanisms operating in these polymerization processes.

Herein, we report the results of a study on the characterization of ternary systems composed of copper, either at the +1 or +2 oxidation state, a polydentate nitrogen ligand and a halide ion in a solvent such as acetonitrile that strongly stabilizes the monovalent state.[37,38] The principal aim of the study is to obtain information on the main species that are present in the reaction medium during polymerization and to contribute to the comprehension of the activation mechanism. To this end, potentiometric, spectrophotometric and cyclic voltammetry measurements were carried out for determining the stability constants of Cu^I and Cu^{II} complexes with the ligands pentamethyldiethylenetriamine (PMDETA) and tris(2-dimethylaminoethyl)amine (Me_6TREN) (Scheme 2), both in the absence and presence of chloride or bromide ions. These two aliphatic polyamines are among the most widely used ligands in ATRP thanks to their commercial availability and the high catalytic activity of their copper complexes.

As will be shown, both binary and ternary systems involve several Cu(II) or Cu(I) species, most of which have not been structurally well characterized. However, X-ray crystallographic data for some Cu complexes with these ligands are reported in the literature.[21] In general, Cu(I) forms tetracoordinated complexes, whereas the most favorable coordination number for Cu(II) is five. Some examples of molecular structures of CuL are schematically illustrated in Scheme 2. For example, Cu^IMe_6TREN has a trigonal pyramidal geometry (Scheme 2a), whereas the structure of $Cu^{II}Me_6$TREN and $XCu^{II}Me_6$TREN is best described as trigonal bipyramidal (Scheme 2b). In contrast, Cu^{II}PMDETA has a square pyramidal geometry (Scheme 2c). In this work, no attempts were made to define the chemical structures of the species involved in the speciation equilibria. We consider, however, tetracoordination and pentacoordination for all Cu(I) and Cu(II) species, respectively.

Experimental Section

Chemicals. Acetonitrile (Carlo Erba, RS) was distilled over CaH_2 and stored under argon atmosphere. Tetraethylammonium tetrafluoroborate ($(C_2H_5)_4NBF_4$, Alfa Aesar, 99%) was recrystallized from ethanol and dried in a vacuum oven at 70 °C for 48 h. Tetraethylammonium chloride (Aldrich, 98%) and tetraethylammonium bromide (Aldrich, 99%) were recrystallized from dichloromethane−acetone−hexane (2:2:1) and ethanol−diethyl ether, respectively, and were dried in a vacuum oven at 70 °C. Tris(2-dimethylaminoethyl)amine (Me_6TREN) was prepared according to a published procedure,[39] by methylation of tris(2-aminoethyl)amine (TREN) in a mixture of formaldehyde and formic acid and was purified by vacuum distillation. Copper(II) trifluoromethanesulfonate (Aldrich, 98%), tetrakis(acetonitrile)copper(I) tetrafluoroborate (Aldrich, 97%) and pentamethyldiethylenetriamine (PMDETA, Alfa Aesar, 98%) were used without further purification. The Cu^{II} salt was standardized by iodometric titration, whereas standardization of Cu^I was carried out by spectrophotometric analysis, using 2,9-dimethyl-1,10-phenanthroline as a specific ligand.[40]

Cyclic Voltammetry. Electrochemical measurements were carried out on a computer-controlled Autolab PGSTAT30 potentiostat (Eco-Chimie, Utrecht, Netherlands). All experiments were carried out at 25 °C in a three-electrode cell system using a glassy carbon (GC) disk (3 mm diameter, Tokay GC20) as a working electrode and a Pt ring as a counter-electrode. The active area of the working electrode ($A = 0.082$ cm^2) was determined by cyclic voltammetry using ferrocene ($D = 2.6 \times 10^{-5}$ cm^2 s^{-1} in CH_3CN + 0.1 M $(C_2H_5)_4NBF_4$)[41] as a redox probe. The reference electrode was a $Ag|AgI|I^-$ electrode built as described previously.[42] The potential of this reference electrode was always measured versus the ferrocenium/ferrocene couple ($E°_{Fc^+/Fc} = 0.391$ V vs SCE in CH_3CN), which was used as an internal standard. This has allowed conversion of the potentials to the aqueous saturated calomel electrode (SCE) scale to which all potentials reported in the paper are referenced. Prior to each experiment the working electrode surface was cleaned by polishing with a 0.25-μm diamond paste, followed by ultrasonic rinsing in ethanol for 5 min.

Potentiometric Titrations. The stability constants of Cu^I complexes with amine ligands and/or halide ions were determined by potentiometric titration of 20 mL of CH_3CN + 0.1 M $(C_2H_5)_4NBF_4$ solutions at 25 °C. Since these complexes are highly unstable in the air, all solutions used in the titrations were prepared in Schlenk volumetric flasks and carefully degassed with Ar ($O_2 < 0.1$ ppm). Furthermore, all measurements were carried out in a Mecaplex drybox. Typical solution volumes and analyte concentrations are reported in the caption of Figure 3.

The indicator electrode was a 3% (w/w) copper amalgam, which was prepared as described in the literature[43] and stored in a Schlenk tube under degassed 0.1 M $HClO_4$. The reference electrode was a $Ag|Ag^+$, 0.01 M in CH_3CN + 0.1 M $(C_2H_5)_4NBF_4$ separated from the working solutions by a porous Vycor tip (Bioanalytical System). Potentiometric data were collected with a Keithley 197A digital multimeter and elaborated by the computer program PITMAP.[44] The program minimizes the sum

of the squares of the differences between experimental and calculated *emf* values. Optimization is performed using pitmapping[45] or simplex[46] as nonlinear least-squares algorithms. Mass balance equations are solved by means of the Newton−Raphson method[46] to obtain the concentrations of all species at equilibrium. The standard reduction potential of the $Cu^{II}(CH_3CN)_4^{2+}/Cu^{I}(CH_3CN)_4^{+}$ couple in acetonitrile was determined by potentiometry using Pt as the indicator electrode.

Spectrophotometric Titrations. The stability constants of Cu^{II} complexes with amine ligands and/or halide ions were determined by spectrophotometric titration in CH_3CN + 0.1 M $(C_2H_5)_4NBF_4$ at 25 °C, using a Varian Cary 5 spectrometer in 10 mm optical path cells. Typical solution volumes and analyte concentrations are reported in the caption of Figure 2. Spectrophotometric data were elaborated by the computer program PITMAP.

Results and Discussion

Determination of Redox Potentials. Cyclic voltammetry (CV) measurements were carried out to determine the formal reduction potentials of the $Cu^{II}S_4^{2+}/Cu^{I}S_4^{+}$ (S = CH_3CN) and $Cu^{II}L^{2+}/Cu^{I}L^{+}$ redox couples. Figure 1 shows examples of cyclic voltammograms of $Cu^{I}S_4^{+}$, recorded in CH_3CN + 0.1 M $(C_2H_5)_4NBF_4$ both in the absence and presence of equimolar amounts of the ligands Me_6TREN and PMDETA. A reversible peak couple attributable to the oxidation of Cu^{I} to Cu^{II} is observed in all cases. It is important to emphasize that CV experiments were carried out also for the Cu^{II} species, but the results were identical with those reported in Figure 1; as expected, the voltammetric behavior of the Cu^{II}/Cu^{I} couple does not depend on the starting species.

The redox reaction underlying the reversible peak couple observed in CV is

$$Cu^{II}L^{2+} + e^- \rightleftarrows Cu^{I}L^{+} \qquad (1)$$

where L stands for Me_6TREN or PMDETA. A similar reaction can be written for the redox reaction involving copper complexes with the solvent. Analysis of the CV responses shows that at low scan rates ($v \le 0.1$ V s^{-1}), the separation between the anodic and cathodic peaks, $\Delta E_p = E_{pa} - E_{pc}$, of the two copper-amine complexes is close to the Nernstian value of 60 mV. By contrast, the $Cu^{II}S_4^{2+}/Cu^{I}S_4^{+}$ couple shows high peak separations even at very low scan rates ($\Delta E_p \approx 200$ mV at $v = 0.05$ V s^{-1}). This points out that the redox process of this couple involves a quasi-reversible electron transfer (ET), whereas the redox behavior of the copper-amine complexes conforms to that of a reversible ET.[47]

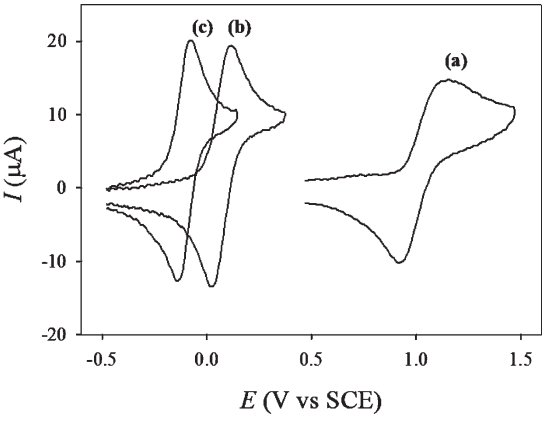

Figure 1. Cyclic voltammetry of $Cu^{I}(CH_3CN)_4BF_4$ in CH_3CN + 0.1 M $(C_2H_5)_4NBF_4$ recorded at $v = 0.05$ V s^{-1} in the absence and presence of nitrogen ligands. Key: (a) 1.04 mM $Cu^{I}(CH_3CN)_4BF_4$; (b) 1.04 mM $Cu^{I}(CH_3CN)_4BF_4$ + 1.04 mM PMDETA; (c) 1.04 mM $Cu^{I}(CH_3CN)_4BF_4$ + 1.04 mM Me_6TREN.

The formal reduction potential of the Cu^{II}−amine complexes can be calculated from the CV data according to the following equation, valid for Nernstian processes:

$$E_{1/2} = \frac{E_{pa} + E_{pc}}{2} = E^{\circ\prime} + \frac{RT}{nF}\ln\left(\frac{D_R}{D_O}\right)^{1/2} \qquad (2)$$

where D_R and D_O are the diffusion coefficients of the reduced and oxidized species, respectively, n is the exchanged number of electrons and F is the Faraday constant. The diffusion coefficients of the Cu^{I} and Cu^{II} complexes can be easily determined from cyclic voltammetry through the Randles-Sevcik equation

$$i_p = 0.4463nFAC^*\left(\frac{nF}{RT}\right)^{1/2} D^{1/2}v^{1/2} \qquad (3)$$

where A is the area of the electrode and C^* is the bulk concentration of the electroactive species. Using a GC electrode of active area $A = 0.082$ cm^2, the diffusion coefficients of Cu^{II} and Cu^{I} complexes were calculated from the peak currents recorded for each species at different scan rates. The values of D obtained for each Cu complex, together with the peak potentials and the formal reduction potentials calculated from eq 2, are reported in Table 1. These data were obtained as the average of the results of at least three independent experiments.

As shown by the CV data reported in Table 1, the $Cu^{II}S_4^{2+}/Cu^{I}S_4^{+}$ redox couple does not undergo a reversible ET, which means that eq 2 cannot be used to calculate the formal reduction potential. In this case, $E^{\circ\prime}_{Cu^{II}/Cu^{I}}$ has been determined by potentiometric measurements, using a Pt indicator electrode. The potential of this electrode is related to the concentrations of Cu^{II} and Cu^{I} through the Nernst equation (eq 4), which reduces to $E = E^{\circ\prime}$ at $C_{Cu^{II}}/C_{Cu^{I}} = 1$. A solution of Cu^{I} was titrated with Cu^{II} to obtain a series of $E_{Cu^{II}/Cu^{I}}$ values for different $C_{Cu^{II}}/C_{Cu^{I}}$ ratios in the range from 0.13 to 2. A plot of $E_{Cu^{II}/Cu^{I}}$ versus $\log(C_{Cu^{II}}/C_{Cu^{I}})$ shows a straight line with an intercept corresponding to $E^{\circ\prime}_{Cu^{II}/Cu^{I}}$. The value of $E^{\circ\prime}_{Cu^{II}/Cu^{I}}$ calculated from the potentiometric titrations (three trials) is included in Table 1.

$$E_{Cu^{II}/Cu^{I}} = E^{\circ\prime}_{Cu^{II}/Cu^{I}} + \frac{2.303RT}{F}\log\frac{C_{Cu^{II}}}{C_{Cu^{I}}} \qquad (4)$$

As is shown in Table 1, the redox potentials of $Cu^{II}L^{2+}/Cu^{I}L^{+}$ are negatively shifted by about 1 V with respect to

Table 1. Thermodynamic Properties of the Cu^{II}/Cu^{I} Redox Couple with Different Ligands in CH_3CN + 0.1 M $(C_2H_5)_4NBF_4$ at T = 25 °C[a]

ligand	E_{pc}[b] (V)	E_{pa}[b] (V)	ΔE_p[b] (mV)	$E_{1/2}$[b] (V)	$10^5 D_{Cu^{II}}$ (cm^2 s^{-1})	$10^5 D_{Cu^{I}}$ (cm^2 s^{-1})	$E^{0\prime c}$ (V)	β^{II}/β^{I}
CH_3CN	0.931	1.129	198				1.056[d]	
PMDETA	0.034	0.105	71	0.070	0.85	1.42	0.063	6.11×10^{16}
Me_6TREN	−0.142	−0.077	65	−0.110	0.81	1.80	−0.120	7.58×10^{19}

[a] Potentials are referenced to SCE. [b] Average of values measured at $v = 0.05$ V s^{-1}. [c] Calculated from eq 2, unless otherwise stated. [d] Determined by potentiometry.

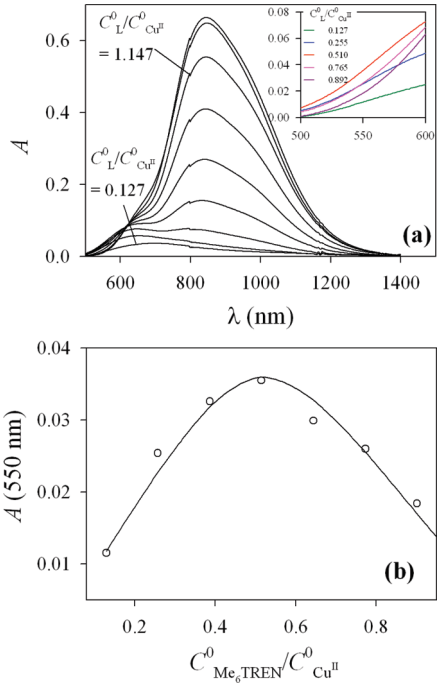

Figure 2. (a) UV−vis spectra of $Cu^{II} + Me_6TREN$ solutions at 25 °C in $CH_3CN + 0.1$ M $(C_2H_5)_4NBF_4$, $V^0 = 5$ mL, $C^0_{Cu^{II}} = 1.187 \times 10^{-3}$ M, step additions of a 7.572×10^{-2} M solution of Me_6TREN. (b) Absorbance values at 550 nm vs. $C^0_{Me_6TREN}/C^0_{Cu^{II}}$, and best-fit curve.

$E^{\circ\prime}_{Cu^{II}/Cu^{I}}$, clearly indicating that the ligands induce a strong stabilization toward the Cu^{II} oxidation state. In other words, the stability constants of $Cu^{II}L^{2+}$ are largely higher than those of $Cu^{I}L^{+}$. The relative stability of the complexes, that is, the ratio of the stability constants, can be calculated from the redox potentials according to eq 5, which has been derived on the basis of a thermochemical cycle based on the relevant redox and complexation reactions.

$$\ln \frac{\beta^{II}}{\beta^{I}} = \frac{F}{RT}(E^{\circ\prime}_{Cu^{II}/Cu^{I}} - E^{\circ\prime}_{Cu^{II}L/Cu^{I}L}) \qquad (5)$$

where β^{II} and β^{I} are the stability constants of $Cu^{II}L^{2+}$ and $Cu^{I}L^{+}$, respectively.

The β^{II}/β^{I} ratios calculated for the two amine ligands are reported in Table 1. These values show that the coordination properties of Cu^{I} strongly differ from those of Cu^{II}, which is much more stabilized by complexation with nitrogen ligands.

Speciation Study. Cu^{II} and Cu^{I} speciation data (number, stoichiometry, and stability constants of the complexes formed in solution) were obtained by means of two different techniques. Cu^{II} complexes display strong absorption bands in the UV and/or in the visible spectral region. Their shape and position depend on the type and number of coordinated ligands. Cu^{I} complexes do not have significant UV−vis absorptions, except those pertaining to the ligands themselves, which change only slightly upon metal complexation. On the other hand, no useful indicator electrode was available for Cu^{II}, whereas a reversible Nernstian copper amalgam electrode can be used to measure the concentration of free Cu^{I}.

For these reasons, Cu^{II} speciation was studied by UV−vis, and data elaboration was performed choosing the wavelengths at which the difference between the absorption of free metal ion, of the binary complexes, and of the ternary ones was a maximum. Figure 2a shows as an example the spectra of $Cu^{II} + Me_6TREN$ solutions in the visible region at several ligand-to-metal ratios. Figure 2b is one of the sets of

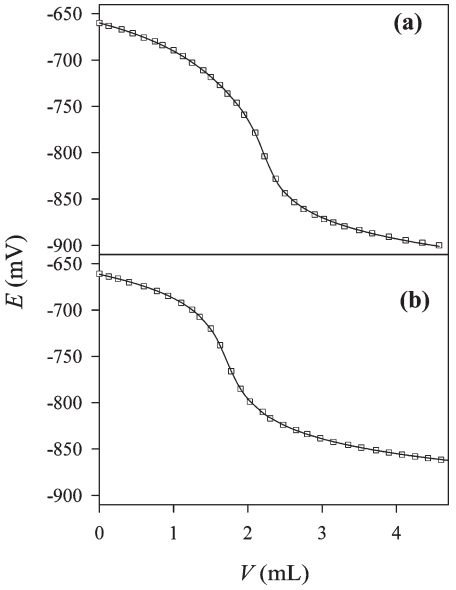

Figure 3. Potentiometric titrations (experimental data and best-fit curves) of $Cu^{I} + L + X$ solutions in $CH_3CN + 0.1$ M $(C_2H_5)_4NBF_4$ at 25 °C. (a) Titration of a solution containing Cu^{I} and Br^- with Me_6TREN, $V^0 = 22.2$ mL ($C^0_{Cu^{I}} = 9.263 \times 10^{-4}$ M, $C^0_{Br^-} = 7.8550 \times 10^{-4}$ M, $C^0_{Me_6TREN} = 9.200 \times 10^{-3}$ M). (b) Titration of a solution containing Cu^{I} and Cl^- with PMDETA, $V^0 = 22.5$ mL ($C^0_{Cu^{I}} = 1.131 \times 10^{-3}$ M, $C^0_{Cl^-} = 1.082 \times 10^{-3}$ M, $C^0_{PMDETA} = 8.873 \times 10^{-3}$ M).

experimental points which were elaborated in order to obtain the speciation in solution.

Cu^{I} speciation was studied by potentiometric titrations. Figure 3 shows two examples of titration curves obtained in this work.

As stated above, the main goal of this paper was to determine the speciation of solutions containing copper (Cu^{II} or Cu^{I}), a polydentate nitrogen ligand L (PMDETA or Me_6TREN) and a halide ion X (Cl^- or Br^-). The elaboration of these systems cannot be performed easily, due to the large number of variables which have to be optimized. These include not only the stability constants of the ternary complexes $Cu_mL_lX_x$, but also those of the binary complexes Cu_mL_l and Cu_mX_x, together with the absorption coefficients ε of all species (for UV−vis measurements) or the calibration parameters of the amalgam electrode (for potentiometric titrations). When the number of variables is excessive (> 5−6), they inevitably become strongly correlated with each other, thus leading to erroneous fitting results.

For this reason, the speciation study was conducted in a sequential manner. As a first step, the binary systems Cu_mX_x and Cu_mL_l were separately investigated, thus obtaining the number, stoichiometry, and stability constants of the binary complexes, and their ε values (for UV−vis measurements). For potentiometric data, a calibration of the electrode was performed before each titration to obtain the apparent E° and to confirm the Nernstian slope. As a second step, the measurements of the ternary systems were performed, and the respective data were elaborated by fixing all variables determined during the first step.

All speciation data obtained for Cu^{II} and Cu^{I} complexes are listed in Table 2. Together with stoichiometry and global stability constants (β), also step stability constants (K) are reported for the step addition of halide ions X. The K values can be easily computed from the corresponding β values, and they represent the tendency by which the given species can add one X.

Binary Copper−Halogen Systems. A large number of works regarding the complexation of Cu^{II} or Cu^{I} with Cl^-

Table 2. Stoichiometry and Stability Constants (Global Constants β and Step Constants K) of Binary and Ternary Complexes formed in CH_3CN Solutions between Copper (Cu^{II} or Cu^{I}), L (PMDETA or Me_6TREN), and X (Cl^- or Br^-) at 25 °C in the Presence of 0.1 M $(C_2H_5)_4NBF_4$

	Cu^{II}		Cu^{I}	
stoichiometry (m,l,x)	log β[a]	log K	log β[a]	log K[b]
	Binary, X = Cl^-			
1,0,1	7.48 ± 0.04	7.48	4.27 ± 0.01	4.27
1,0,2	13.31 ± 0.04	5.83	9.72 ± 0.01	5.45
1,0,3	19.22 ± 0.06	5.91		
1,0,4	22.47 ± 0.05	3.25		
	Binary, X = Br^-			
1,0,1	6.3 ± 0.1	6.3	3.54 ± 0.01	3.54
1,0,2	11.3 ± 0.1	5.0	7.30 ± 0.01	3.76
1,0,3	14.8 ± 0.1	3.5		
1,0,4	17.9 ± 0.1	3.1		
	Binary, L = PMDETA			
1,1,0	23.3 ± 0.1[c]		6.53 ± 0.01	
1,2,0	28.09 ± 0.03		8.43 ± 0.09	
2,1,0	25.10 ± 0.03		8.34 ± 0.07	
	binary, L = Me_6TREN			
1,1,0	27.2 ± 0.1[c]		7.33 ± 0.01	
1,2,0	30.38 ± 0.01		9.64 ± 0.02	
2,1,0	31.13 ± 0.02		9.23 ± 0.05	
	Ternary, L = PMDETA, X = Cl^-			
1,1,1	28.85 ± 0.03	5.65	8.3 ± 0.2	1.77
1,1,2	32.06 ± 0.02	3.21		
2,1,1			13.7 ± 0.1	5.36
2,1,2			18.76 ± 0.07	5.06
	Ternary, L = PMDETA, X = Br^-			
1,1,1	27.74 ± 0.04	4.54	8.35 ± 0.03	1.82
1,1,2	29.72 ± 0.04	1.98		
2,1,1			12.41 ± 0.06	4.07
	Ternary, L = Me_6TREN, X = Cl^-			
1,1,1	33.8 ± 0.1	6.8	9.90 ± 0.03	2.57
1,1,2	35.0 ± 0.1	1.2		
2,1,1			15.48 ± 0.06	6.25
2,1,2			19.6 ± 0.1	4.12
	Ternary, L = Me_6TREN, X = Br^-			
1,1,1	33.1 ± 0.1	6.1	9.60 ± 0.01	2.27
2,1,1			13.80 ± 0.08	4.57
2,1,2			17.37 ± 0.02	3.57

[a] Values of β refer to reactions: $mCu + lL + xX \rightleftharpoons Cu_mL_lX_x$; uncertainty as ±1 σ, obtained by the fitting procedure. [b] Values of K refer to reactions: $Cu_mL_lX_{x-1} + X \rightleftharpoons Cu_mL_lX_x$. [c] Value obtained combining β^{II}/β^{I} (Table 1) and log β value of $Cu^{I}L^+$; uncertainty was estimated by error propagation.

or Br^- is reported in the literature. It was anyway necessary to perform the complexation studies of binary Cu-X solutions in this work because almost all literature data were obtained in solvents and/or ionic strengths that are different from those adopted in the present study (CH_3CN, 0.1 M $(C_2H_5)_4NBF_4$). When data exist in a similar medium, they were considered to check the accuracy of our results.

All solutions showed the presence of only mononuclear CuX_x complexes, where x = 1, 2, 3, 4 for Cu^{II}, and x = 1, 2 for Cu^{I}. These qualitative results fully agree with the literature.[48] As regards Cu^{I}+X, our quantitative data very closely agree with literature data,[37,43,49,50] in particular those reported by Tagesson et al.,[37] who worked in the same medium as ours, i.e. same solvent, ionic strength and supporting electrolyte. For $Cu^{I} + Cl^-$ they found log $\beta(Cu^{I}Cl)$ = 4.35 and log $\beta(Cu^{I}Cl_2^-)$ = 9.69, which differ from our values by less than 0.1 log units. For $Cu^{I} + Br^-$ they obtained log $\beta(Cu^{I}Br)$ = 3.37 and log $\beta(Cu^{I}Br_2^-)$ = 7.20, which too are very close to our values (Δ log units less than 0.2). Concerning Cu^{II} + Cl, there are a few discordant β values in the literature. Manahan and Iwamoto,[50] who worked in CH_3CN + 0.1 M $(C_2H_5)_4NClO_4$, which is slightly different than our reaction medium, report log β values of 9.7, 17.6, 24.7, and 28.4 for $Cu^{II}Cl^+$, $Cu^{II}Cl_2$, $Cu^{II}Cl_3^-$, and $Cu^{II}Cl_4^{2-}$, respectively. On the other hand, Ishiguro et al.,[51] who worked in the same medium, report the following values of log β: 9.76, 17.31, 19.22, and 22.47 for $Cu^{II}Cl^+$, $Cu^{II}Cl_2$, $Cu^{II}Cl_3^-$, and $Cu^{II}Cl_4^{2-}$, respectively. Both these series of data are significantly larger than ours.

As regards the Cu^{II}+Br^- system, it is well-known that CH_3CN solutions containing Cu^{II} and Br^- are thermodynamically unstable due to the slow auto-oxidation of Br^- by Cu^{II}.[52] We checked the extent of this reaction by collecting UV−vis spectra at various ligand-to-metal ratios and after different mixing times. In our conditions, the auto-oxidation is slow enough to give reproducible UV−vis spectra if Br^- is in stoichiometric excess. Therefore, we were able to perform the complexation study and to obtain stoichiometry and stability constants of the Cu^{II}−Br^- complexes working at $C^0_{Br^-}/C^0_{Cu^{II}} > 1$. However, the absence of data at $C^0_{Br^-}/C_{0Cu^{II}} < 1$ impaired the uncertainty of the stability constant of $Cu^{II}Br^+$ and, as a consequence, of the other stability constants, which therefore have relatively high uncertainties.

In general, both Cu^{II} and Cu^{I} form stronger complexes with Cl^- than with Br^-: there is a difference of about 1 order of magnitude between the corresponding K values. The Cu^{II} complex $Cu^{II}Cl_3^-$ is relatively very stable, as K_3 is practically identical to K_2, and $Cu^{II}Cl_4^{2-}$ is much less stable, as K_4 is almost 3 orders of magnitude lower than K_3. For the Cu^{II} + Br^- system, K values show a more "normal" behavior, smoothly decreasing upon increasing the number of bromide ions. As regards Cu^{I}, both $Cu^{I}Cl_2^-$ and $Cu^{I}Br_2^-$ are relatively more stable than the corresponding monohalide complexes: K_2 is significantly larger than K_1, especially in the case of Cl^-. These general considerations are in agreement with all results reported in the literature referring to CH_3CN as a solvent (see, e.g., citations in ref 50).

Binary Copper-PMDETA Systems. Very few papers regarding Cu^{II}− and Cu^{I}−PMDETA complexation studies are available in the literature, and all of these works were performed using water as a solvent. The complexes detected in aqueous solutions were only $Cu^{II}L^{2+}$, $Cu^{II}LH_{-1}^{+}$ and $Cu^{I}L^+$ (L = PMDETA).[48] This speciation was not confirmed by us in CH_3CN, where the formation of additional complexes having metal-to-ligand stoichiometry 1:2 and 2:1 was observed for both Cu^{II} and Cu^{I}. Thus, in CH_3CN a second ligand molecule can add to the metal center, or a second metal ion can add to the ligand moiety.

As regards Cu^{II} + PMDETA, plots of absorbance vs. $C^0_{PMDETA}/C^0_{Cu^{II}}$ ratio clearly indicate the formation of the complex $Cu^{II}L^{2+}$. Figure 4 reports an example of an absorbance vs. $C^0_{PMDETA}/C^0_{Cu^{II}}$ plot for a titration of Cu^{II} with PMDETA. The absorbance increases linearly with the concentration ratio as long as $C^0_{PMDETA}/C^0_{Cu^{II}} < 1$, giving a sharp maximum at $C^0_{PMDETA}/C^0_{Cu^{II}} = 1$. Unfortunately, the sharpness of the maximum does not allow to obtain a reliable constant for $Cu^{II}L^{2+}$, as the experimental points can be fitted by any log $\beta_{1,1,0}$ value larger than *ca.* 8. In other

words, the relative weakness of CH_3CN solvation, together with the strength of PMDETA as a Cu^{II} ligand, does not allow the direct determination of the stability constant of $Cu^{II}L^{2+}$ by UV−vis, even in the most favorable experimental conditions (e.g., very low metal and ligand concentrations). For this reason, the stability constant of this complex was obtained by calculation, through the potentiometric $\beta_{1,1,0}$ value of $Cu^{I}L^{+}$ and the voltammetric β^{II}/β^{I} ratio (see previous section). Once the log β value for $Cu^{II}L^{2+}$ was determined in this way, spectrophotometric data allowed to determine the stability constants of $Cu_2^{II}L^{4+}$ and $Cu^{II}L_2^{2+}$. These two species had to be included in the speciation model to better fit the absorbance data. Parts a and b of Figure 5 display the distribution diagrams of Cu^{II}- and Cu^{I}−PMDETA solutions drawn at a metal concentration of 10^{-3} M.

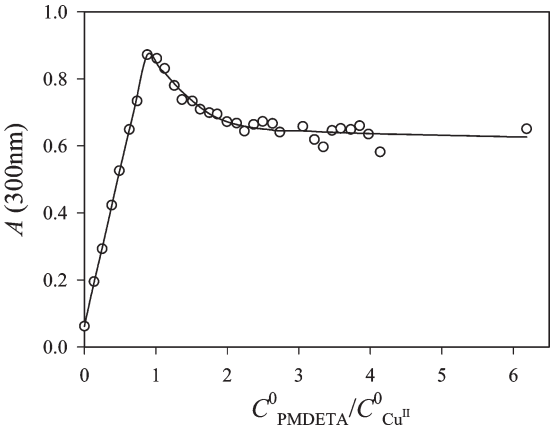

Figure 4. Variation of absorbance (experimental data and best-fit curve) of solutions containing Cu^{II} and PMDETA, measured at 300 nm in CH_3CN+0.1 M $(C_2H_5)_4NBF_4$ at 25 °C, as a function of $C^0_{PMDETA}/C^0_{Cu^{II}}$. $V^0 = 5$ mL; $C^0_{Cu^{II}} = 1.491\times10^{-4}$ M.

As usual, diagrams are plotted vs. the cologarithm of the concentration of free ligand (pL).

Binary Copper−Me$_6$TREN Systems. Similarly as for PMDETA, Cu-Me$_6$TREN complexes having metal-to-ligand stoichiometry of 1:1, 1:2, and 2:1 were detected for both Cu^{II} and Cu^{I}. The presence of $Cu^{II}_2L^{4+}$ was confirmed by the UV−vis spectra, as this complex has a specific absorption at $\lambda \approx 550$ nm (Figure 2a), which is sufficiently resolved from the other bands. Figure 2b illustrates the variation of the absorbance at 550 nm as a function of $C^0_{Me_6TREN}/C^0_{Cu^{II}}$. As shown, the absorbance increases to a maximum value at $C^0_{Me_6TREN}/C^0_{Cu^{II}} = 0.5$, which corresponds to the ideal condition for the maximum yield of the bimetallic complex. No support to this stoichiometry can be obtained from the literature, as the few published papers regarding Cu^{II}−Me$_6$TREN complexation were performed using water as a solvent, and the only complex detected in those conditions has a 1:1 stoichiometry.[48] The strength of Me$_6$TREN as a Cu^{II} ligand in CH_3CN did not allow the direct determination of the stability constant of $Cu^{II}L^{2+}$ from the UV−vis spectra: this value was obtained by calculation as described above for PMDETA.

No speciation data are reported in the literature for the Cu^{I}−Me$_6$TREN system, too. Indeed, the Ag^{I}−Me$_6$TREN system in DMSO has recently been studied by Tolazzi et al.,[53] who detected the metal−ligand species $Ag^{I}L^{+}$, $Ag^{I}L_2^{+}$, and $Ag^{I}_2L^{2+}$, which have the same stoichiometry as our complexes. Not only do Cu^{I}− and Ag^{I}−Me$_6$TREN solutions contain the same complexes but also (and surprisingly) these species have very similar stability constants (log β values given by Tolazzi: 7.63, 9.06, and 9.21 for $Ag^{I}L^{+}$, $Ag^{I}L_2$, and $Ag_2^{I}L^{2+}$, respectively). Figures 5c and 5d display the distribution diagrams of Cu^{II}- and Cu^{I}-Me$_6$TREN solutions. The diagrams and the log β values indicate that Me$_6$TREN is a stronger binder for Cu^{II} and Cu^{I} than PMDETA: this was expected because an additional nitrogen

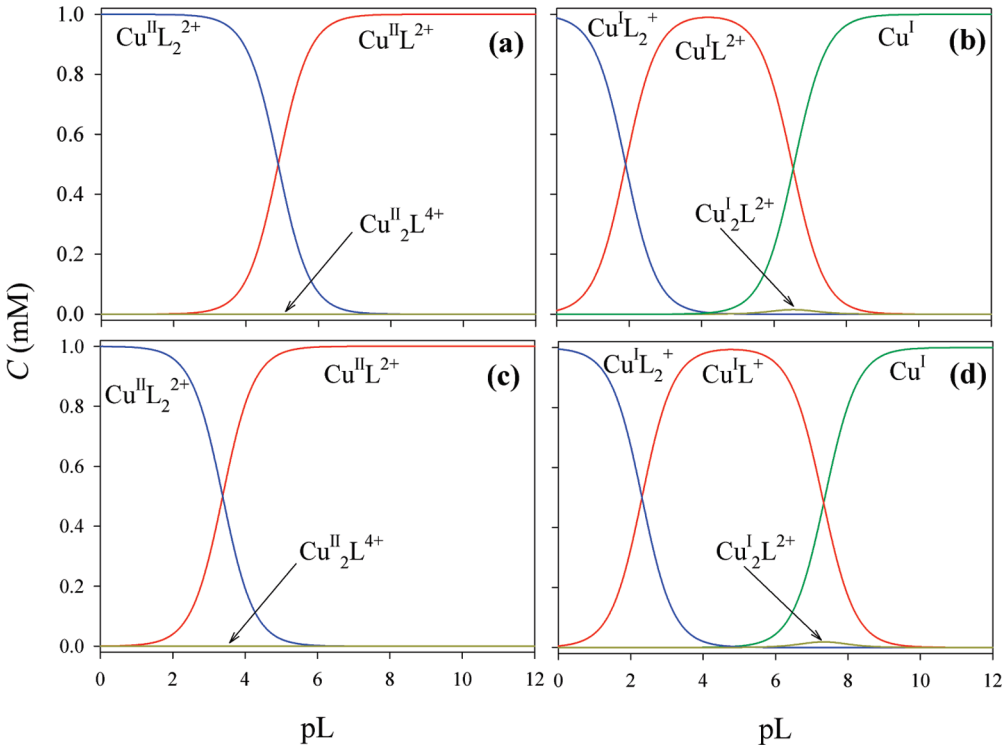

Figure 5. Distribution diagrams vs. free ligand concentration (L = PMDETA or Me$_6$TREN) of binary Cu−L systems, $T = 25$ °C in CH_3CN + 0.1 M $(C_2H_5)_4NBF_4$, $C^0_{Cu} = 10^{-3}$ M. Key: (a) Cu^{II} + PMDETA, (b) Cu^{I} + PMDETA, (c) Cu^{II} + Me$_6$TREN, (d) Cu^{I} + Me$_6$TREN.

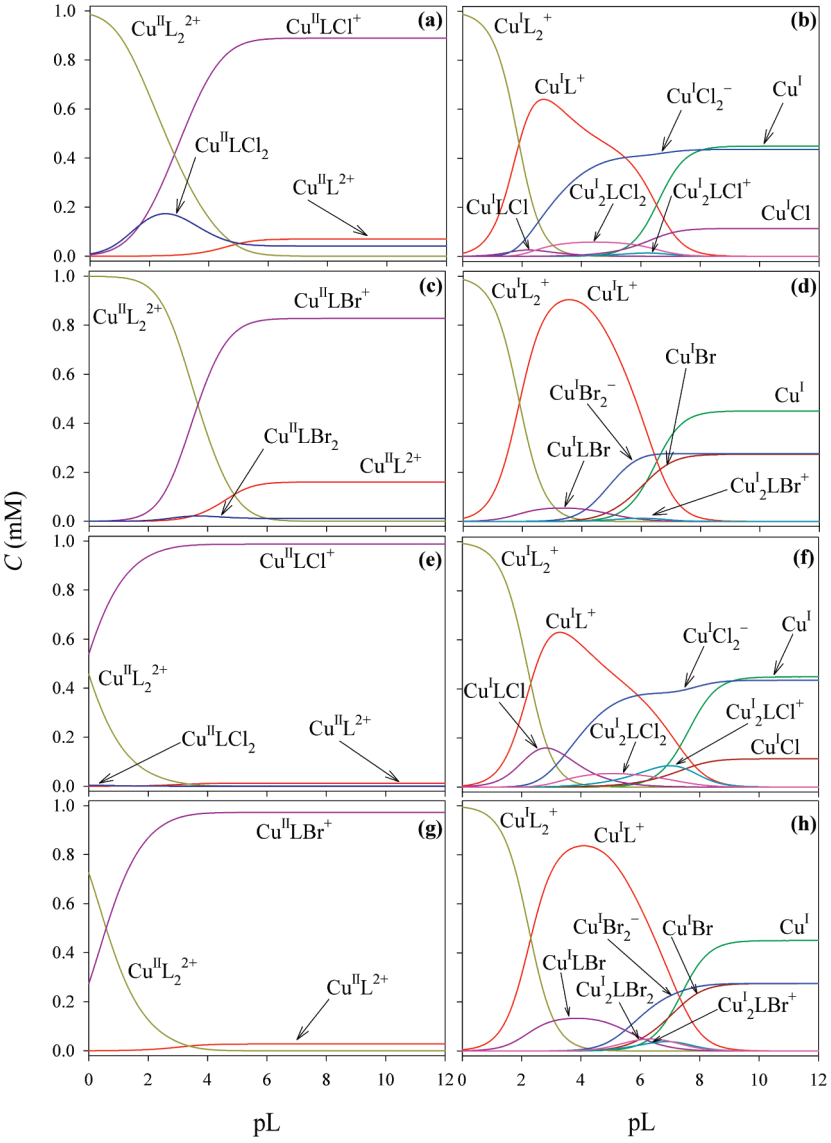

Figure 6. Distribution diagrams vs. free ligand concentration (L = PMDETA or Me_6TREN) of Cu-L-X species (X = Cl^- or Br^-), T = 25 °C in CH_3CN + 0.1 M $(C_2H_5)_4NBF_4$, $C^0_{Cu} = C^0_X = 10^{-3}$ M. Key: (a) Cu^{II} + PMDETA + Cl^-, (b) Cu^I + PMDETA + Cl^-, (c) Cu^{II} + PMDETA + Br^-, (d) Cu^I + PMDETA + Br^-, (e) Cu^{II} + Me_6TREN + Cl^-, (f) Cu^I + Me_6TREN + Cl^-, (g) Cu^{II} + Me_6TREN + Br^-, (h) Cu^I + Me_6TREN + Br^-.

is available in Me_6TREN for the metal coordination. The most stabilized complexes are the CuL- and Cu_2L-type ones.

Ternary Copper−PMDETA−Halogen Systems. Assuming that PMDETA binds Cu^{II} through its three nitrogen atoms, the remaining free coordination sites of the metal ion can be engaged in the coordination of one or more halogen ions. For Cu^{II}−PMDETA−X systems the species $Cu^{II}LX^+$ and $Cu^{II}LX_2$ were detected. The addition of the first halogen to $Cu^{II}L^{2+}$ is less favored than the same halogen addition to the free metal ion. In fact, for the binary complexes $Cu^{II}X^+$, log K_1 = 7.48 and 6.3 for X = Cl^- and Br^-, respectively, whereas the corresponding log K_1 values found for $Cu^{II}LX^+$ are 5.65 and 4.54. Steric considerations, and/or the minor acidic properties of $Cu^{II}L^{2+}$ with respect to free Cu^{II}, can justify this result. The same is true for the formation of $Cu^{II}LCl_2$ (log K_2 = 3.21, that of $Cu^{II}Cl_2$ is 5.83) and $Cu^{II}LBr_2$ (log K_2 = 1.98, that of $Cu^{II}Br_2$ is 5.0). $Cu^{II}LCl_2$ has been isolated in the solid state and crystallographically characterized.[54] Parts a and c of Figure 6 display the distribution diagrams of Cu^{II}−PMDETA−X solutions, where both Cu^{II} and X stoichiometric concentrations are 10^{-3} M. In this condition, the ternary complex $Cu^{II}LX^+$ is the predominating species over a wide pL range.

Ternary Cu^I−PMDETA−X systems display a different speciation: complexes bearing two metal ions form in solution. These complexes can be considered as the product of a halogen binding to the $Cu^I_2L^{2+}$ species, and they are more stable than the mononuclear Cu^ILX (for both Cl^- and Br^- this complex has a very low log K value). Log K values for $Cu^I_2LCl^+$ and $Cu^I_2LCl_2$ are 5.36 and 5.06, respectively, indicating that the addition of a second chloride is comparably as favorable as that of the first one. This result resembles what was found for the binary Cu^I−Cl^- system (see above). For Br^-, only one dinuclear ternary complex was detected, most likely because Cu^I is more weakly bound by Br^- than by Cl^-. In fact, $Cu^I_2LBr^+$ is 1 order of magnitude less stable than $Cu^I_2LCl^+$. In the case of Cu^{II}, these dinuclear species were not detected probably because $Cu^{II}_2L^{4+}$ is less stable than $Cu^I_2L^{2+}$. Parts b and d of Figure 6 display the distribution diagrams of Cu^I−PMDETA−X solutions. Differently than for Cu^{II}, for Cu^I the ternary species are not the main species in solution at any pL value, and there is a more complicated speciation pattern, as several binary Cu^I−PMDETA and Cu^I−X species have a significant concentration at the given conditions.

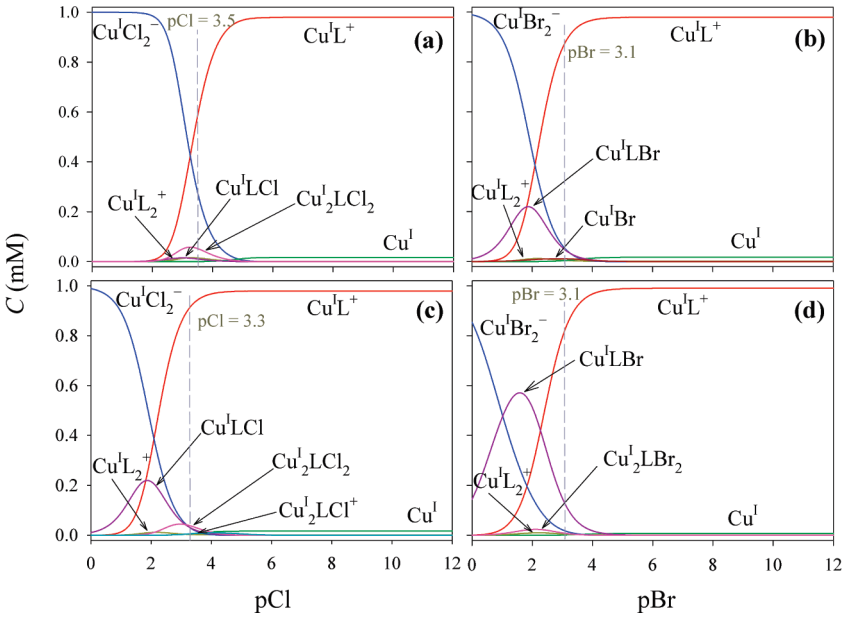

Figure 7. Distribution diagrams vs. free halogen ion concentration (pCl or pBr) of ternary $Cu^I + L + X$ systems in CH_3CN + 0.1 M $(C_2H_5)_4NBF_4$ at 25 °C, $C^0_{Cu^I} = C^0_L = 10^{-3}$ M. Key: (a) Cu^I + PMDETA + Cl^-, (b) Cu^I + PMDETA + Br^-, (c) Cu^I + Me_6TREN + Cl^-, (d) Cu^I + Me_6TREN + Br^-.

Ternary Copper−Me$_6$TREN−Halogen Systems. Speciation results obtained for Cu−Me_6TREN−X systems are similar to those of Cu−PMDETA−X. For Cu^{II}−Me_6TREN−Cl^- the same species $Cu^{II}LCl^+$ and $Cu^{II}LCl_2$ were detected, but $Cu^{II}LCl_2$ is not as important as it was for PMDETA: its log K is only 1.2, which is much lower than the corresponding value for PMDETA (log K = 3.21). The bromide ternary species $Cu^{II}LBr_2$ was even not detectable. In other words, the addition of a second X and the formation of $Cu^{II}LX_2$ is less favored for Me_6TREN than for PMDETA. This result can be justified considering that Me_6TREN is tetradentate, whereas PMDETA is tridentate. The addition of a second halogen ion to a metal center bound to a tetradentate ligand is more difficult, since probably one of the four Cu^{II}−L energetic coordination bonds must disrupt to allow a second halogen ion to bind to the metal center. This latter occurrence is sometimes described in the literature[55,56] when halogen atoms compete with tetradentate nitrogen ligands for the binding to a metal center. On the other hand, $Cu^{II}LX^+$ is comparably more stable for Me_6TREN than for PMDETA: the observed log K values are 6.8 (for Cl^-) and 6.1 (for Br^-) for Me_6TREN and 5.65 (for Cl^-) and 4.54 (for Br^-) for PMDETA. Parts e and g of Figure 6 display the distribution diagrams of Cu^{II}−Me_6TREN−X solutions: it is evident that the ternary complex $Cu^{II}LX^+$ is practically the only species present in solution over a very wide pL range.

Ternary Cu^I−Me_6TREN−X systems display a similar speciation as Cu^I−PMDETA−X: here too the formation of complexes bearing two metal ions was observed. $Cu^I_2LX_2$ is less important than for PMDETA, as its Cl^- and Br^- step stability constants are much lower than those of $Cu^I_2LX^+$. On the other hand, the latter complex is more stable for Me_6TREN than for PMDETA (e.g., as regards Cl^-, log K = 6.25 instead of 5.36). Parts f and h of Figure 6 display the distribution diagrams of Cu^I−Me_6TREN−X solutions. A relatively complicated speciation and a number of coexisting species at almost any pL value can be observed.

Ternary Cu−L−X Systems. Role of Halide Ions. Figure 6 illustrates how the speciation of copper in a solution containing equimolar amounts of Cu^I or Cu^{II} and X is affected by the concentration of the polyamine ligand L. It clearly shows that while $Cu^{II}LX^+$ is the only relevant species in solution for a wide range of pL values, isolation of a single Cu^I complex, if at all possible, can be achieved only in a very narrow range of pL. These speciation diagrams, however, do not give a clear picture of the most likely distribution in a copper-catalyzed ATRP process. Typically, the catalyst system of an ATRP process consists of a mixture of Cu^IX and L at an initial Cu^I/X/L stoichiometric ratio of 1:1:1. While the metal-to-amine ligand remains constant during the polymerization reaction, the C_X/C_{Cu^I} ratio may increase because of the termination reactions (see Scheme 1). It is very likely that speciation of Cu^I strongly affects the kinetics of the activation step, i.e., reaction of Cu^I with the dormant species. It is therefore interesting to construct speciation diagrams for Cu^I, using a fixed Cu^I/L ratio (1:1) and a variable concentration of X.

Figure 7 shows Cu^I distribution diagrams vs pX, calculated for both Me_6TREN and PMDETA at $C^0_{Cu^I} = C^0_L = 10^{-3}$ M. Although these diagrams are less complicated than those of Figure 6 for the polyamine ligands, they evidence a strong dependence of Cu^I distribution on pX. As shown, Cu^I speciation depends on both the nature of the ligand and type of halide ion, the latter showing a more marked effect. In all cases, the most relevant species are Cu^IL^+, $Cu^IX_2^-$, and Cu^ILX, except for the Cu^I + PMDETA + Cl^- system in which only the first two species are important as they account for at least 95% of the whole Cu^I at all pCl values. For all systems, the binary $Cu^IX_2^-$ complex is the predominant species at low pX values, whereas Cu^IL^+ predominates at high pX values. In particular, Cu^IL^+ has a wider range of stability in the case of bromide for both polyamine ligands, which reflects the major affinity of chloride ion for the metal center and its ability of generating strong binary Cu^IX_n complexes. The role of the ternary complex Cu^ILX depends on both the ligand type and the halide ion. This species is more important for Me_6TREN than for PMDETA; also the complex with Br^- is more important than that of Cl^-.

The vertical lines in Figure 7 show the equilibrium distribution at the beginning of a typical ATRP experiment. In all cases the predominant species in this circumstance is the binary Cu^IL^+ complex rather than Cu^ILX, which is sometimes assumed to be the active catalyst. Indeed, the standard reduction potential of Cu^ILX is about 0.16−0.25 V more

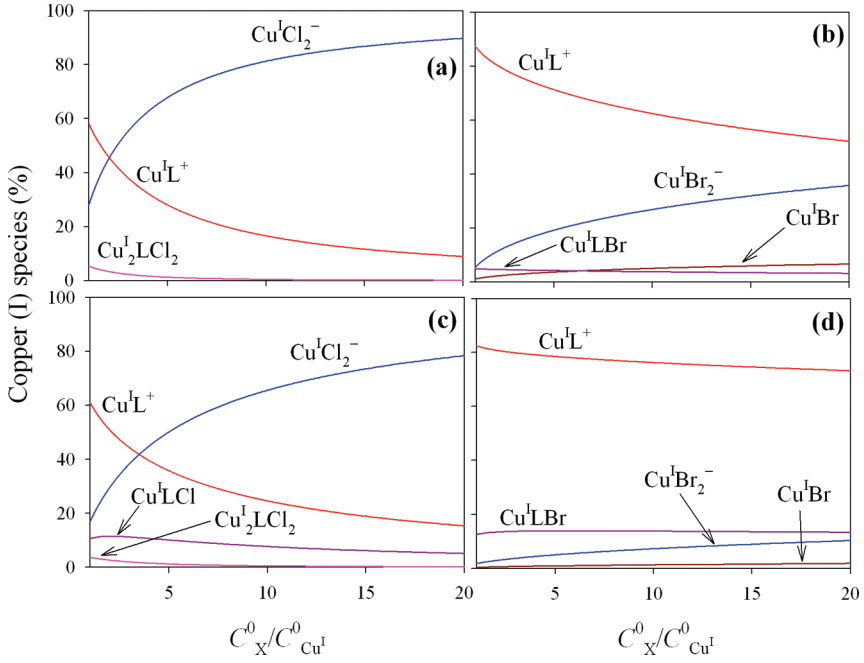

Figure 8. Dependence of the distribution of the most relevant species for the ternary system Cu^I/L/X in CH_3CN + 0.1 M $(C_2H_5)_4NBF_4$ at 25 °C on the $C^0_X/C^0_{Cu^I}$ ratio. Key: (a) Cu^I + PMDETA + Cl^-, (b) Cu^I + PMDETA + Br^-, (c) Cu^I + Me_6TREN + Cl^-, (d) Cu^I + Me_6TREN + Br^-; calculations were carried out at $C^0_X = C^0_L = 10^{-3}$ M and variable $C^0_{Cu^I}$ from 10^{-3} M down to 5×10^{-5} M.

negative than that of Cu^IL^+, which, on thermodynamic grounds, makes the former a more stronger reducing agent than the latter.[57]

If during polymerization $Cu^{II}LX^+$ is accumulated because of the termination reactions, the ratio between the total X and Cu^I concentrations increases, which modifies the distribution diagrams shown in Figure 7.

To put the effect of changing C_X/C_{Cu^I} into quantitative terms, we calculated the equilibrium concentrations of all pertinent species for a series of concentration ratios. We started with a solution containing Cu^I, L and X, each at a concentration of 10^{-3} M. Then, according to the ATRP equilibrium, we considered that Cu^I reacts with an initiator RX to produce Cu^{II} with a very low equilibrium constant,[17] so that the catalyst is almost quantitatively present as Cu^I. However, during the ATRP process a progressively increasing amount of Cu^{II} does not go back to Cu^I because of the termination reactions. This is equivalent to decreasing the overall concentration of Cu^I by some amount, say y, and increasing that of the halide ion by the same amount. Thus, during the ATRP process the total concentrations (in mol dm^{-3}) can be expressed as $C^0_{Cu^I} = 10^{-3} - y$ and $C^0_X = 10^{-3} + y$. Using these new concentrations, which are considered as the initial values for a new equilibrium, we calculated the distribution of Cu^I. In this calculation we took into consideration the presence of Cu^{II} at a concentration of y M.

The above-described calculation has been repeated for a large number of y values and the resulting distribution values were plotted versus $C^0_X/C^0_{Cu^I}$ (Figure 8), which is calculated as $10^{-3}/(10^{-3} - y)$. These distribution diagrams clearly show that Cu^I speciation is strongly affected by $C^0_X/C^0_{Cu^I}$, especially when X = Cl^- and L = PMDETA. The most important species present in solution for all four combinations are Cu^IL^+ and $Cu^IX_2^-$; Cu^ILX is always present as a small fraction (< 15%) and is not very much affected by $C^0_X/C^0_{Cu^I}$. In general, increasing $C^0_X/C^0_{Cu^I}$ favors the formation of $Cu^IX_2^-$ over Cu^IL^+, but the competition between the two species depends on the nature of X. When X = Cl^-, $Cu^IX_2^-$ becomes the predominant species at $C^0_X/C^0_{Cu^I} \approx 2.5$ and 4 for L = PMDETA and Me_6TREN, respectively. When instead X = Br^-, Cu^IL^+ remains the predominant species up to $C^0_X/C^0_{Cu^I} = 20$. A case of particular interest is represented by the ternary system Cu^I+Me_6TREN+Br^-. The composition of this system is almost unaffected by $C^0_X/C^0_{Cu^I}$, the predominant species being Cu^IL^+, which remains about 80% for a wide range of $C^0_X/C^0_{Cu^I}$ values.

The distribution diagrams shown above point out that Cu^I always exists in ATRP conditions as a multiplicity of species arising from a complex set of equilibria involving both binary and ternary systems as well as mononuclear and binuclear complexes. Although so far the role of Cu^I speciation in ATRP has never been considered, it is certainly important in the rationalization of the activation mechanism. It is reasonable to assume that some of the possible Cu^I species are not active catalysts or at least do not have the same catalytic activity. In particular, on the basis of the standard reduction potentials of the Cu^{II}/Cu^I couple (see Table 1),[57b] $Cu^IX_2^-$ is expected to be much less active than either Cu^IL^+ or Cu^ILX. As shown in Figure 8 the fraction of Cu^I present as $Cu^IX_2^-$ is expected to increase during polymerization and this will represent a setback for the kinetics of activation of the dormant species and perhaps of the overall process. The speciation and distribution diagrams should depend not only on ligand and halide but also on temperature and medium, as solvent must play a very important role in competitive complexation/solvation of both Cu^I and Cu^{II} species. For example, much slower rate of ATRP of 2-hydroxyethyl methacrylate in protic media was observed in the presence of tetraalkylammonium halides.[58] The slower rate could be ascribed to stronger association of halide anions with Cu^{II} species and increased concentration of deactivating X−Cu^{II} species but also to the decreased concentration of activating Cu^IL^+ species.

Conclusions

The standard reduction potentials of Cu^{II} and $Cu^{II}L$ as well as the global and step stability constants (β and K) of all complexes

arising from the binary Cu−X or Cu−L and ternary Cu−L−X systems have been determined in $CH_3CN + 0.1$ M $(C_2H_5)_4NBF_4$. The binary Cu−X systems show only mononuclear CuX_x complexes, where $x = 1, 2, 3, 4$ for Cu^{II}, and $x = 1, 2$ for Cu^{I}. Both Cu^{II} and Cu^{I} are characterized by high $\log \beta$ values, but the affinity of Cu^{I} for halide ions is considerably smaller than that of Cu^{II}. The binary Cu−L systems form both mononuclear complexes CuL_l, where $l = 1$ or 2, and dinuclear complexes Cu_2L. For both types of complex, Me_6TREN is a much better ligand than PMDETA, especially for Cu^{II}. This is most likely due to the presence of an additional nitrogen in Me_6TREN with respect to the tridentate PMDETA. The ternary systems give rise to a mixture of mononuclear and dinuclear complexes $Cu_mL_lX_x$. Besides CuLX, Cu^{II} gives one more mononuclear species $Cu^{II}LX_2$, whereas Cu^{I} forms dinuclear complexes $Cu^{I}_2LX^+$ and $Cu^{I}_2LX_2$. The halidophilicity of both Cu^{II} and Cu^{I} significantly decreases upon complexation with the polyamine ligands.

Speciation diagrams of the ternary systems show that while there is a wide range of conditions for the predominance of $Cu^{II}LX^+$, Cu^{I} is always present as a mixture of $Cu^{I}L^+$, $Cu^{I}L_2^+$, $Cu^{I}X_2^-$, $Cu^{I}LX$, Cu^+, $Cu^{I}X$, and $Cu^{I}_2LX_2$, with a distribution strongly depending on the concentration of the ligands. In any case, the fraction of dinuclear complexes never exceeds 10%. Analysis of the speciation equilibria as a function of C_X/C_{Cu^I} ratio, which varies during ATRP, reveals interesting insights into the activation step of the process. In fact, this analysis shows that the most important species present in solution are $Cu^{I}L^+$ and $Cu^{I}X_2^-$, whereas the contribution of $Cu^{I}LX$ never exceeds 15% and is little affected by C_X/C_{Cu^I}. In addition, the fraction of $Cu^{I}L^+$, which probably is much more active than $Cu^{II}X_2^-$ at least on thermodynamic grounds, decreases during polymerization while that of the less active species $Cu^{II}X_2^-$ increases. This is detrimental to the activation step and to the overall ATRP process, which may come to a halt long before quantitative conversion of the monomer is achieved. The competition between $Cu^{I}L^+$ and $Cu^{II}X_2^-$ depends on the nature of L and X. When $X = Br^-$, $Cu^{I}L^+$ remains the predominant species even at very high values of C_X/C_{Cu^I}. Thus, using bromides instead of chlorides appears to be more beneficial from the viewpoint of synthesis.

Acknowledgment. This work was supported by the University of Padova through Grant CPDA083370.

References and Notes

(1) Braunecker, W. A.; Matyjaszewski, K. *Prog. Polym. Sci.* **2007**, *32*, 93–146.
(2) Wang, J.-S.; Matyjaszewski, K. *J. Am. Chem. Soc.* **1995**, *117*, 5614–5615.
(3) Kato, M.; Kamigaito, M.; Sawamoto, M.; Higashimura, T. *Macromolecules* **1995**, *28*, 1721–1723.
(4) Matyjaszewski, K.; Xia, J. *Chem. Rev.* **2001**, *101*, 2921–2990.
(5) Kamigaito, M.; Ando, T.; Sawamoto, M. *Chem. Rev.* **2001**, *101*, 3689–3746.
(6) Matyjaszewski, K.; Tsarevsky, N. V. *Nature Chem.* **2009**, *1*, 276–288.
(7) Guliashvili, T.; Percec, V. *J. Polym. Sci., Part A: Polym. Chem.* **2007**, *45*, 1607–1618.
(8) Tang, W.; Tsarevsky, N. V.; Matyjaszewski, K. *J. Am. Chem. Soc.* **2006**, *128*, 1598–1604.
(9) Ouchi, M.; Terashima, T.; Sawamoto, M. *Chem. Rev.* **2009**, *109*, 4963–5050.
(10) Braunecker, W. A.; Brown, W. C.; Morelli, B. C.; Tang, W.; Poli, R.; Matyjaszewski, K. *Macromolecules* **2007**, *40*, 8576–8585.
(11) Pintauer, T.; Matyjaszewski, K. *Chem. Soc. Rev.* **2008**, *37*, 1087–1097.
(12) Jakubowski, W.; Min, K.; Matyjaszewski, K. *Macromolecules* **2006**, *39*, 39–45.
(13) Jakubowski, W.; Matyjaszewski, K. *Angew. Chem.* **2006**, *45*, 4482–4486.
(14) Matyjaszewski, K.; Jakubowski, W.; Min, K.; Tang, W.; Huang, J.; Braunecker, W. A.; Tsarevsky, N. V. *Proc. Natl. Acad. Sci. U.S.A.* **2006**, *103*, 15309–15314.
(15) Tsarevsky, N. V.; Matyjaszewski, K. *Chem. Rev.* **2007**, *107*, 2270–2299.
(16) Tang, W.; Matyjaszewski, K. *Macromolecules* **2006**, *39*, 4953–4959.
(17) Tang, W.; Kwak, Y.; Braunecker, W.; Tsarevsky, N. V.; Coote, M. L.; Matyjaszewski, K. *J. Am. Chem. Soc.* **2008**, *130*, 10702–10713.
(18) Seeliger, F.; Matyjaszewski, K. *Macromolecules* **2009**, *42*, 6050–6055.
(19) Pintauer, T.; Reinöhl, U.; Feth, M.; Bertagnolli, H.; Matyjaszewski, K. *Eur. J. Inorg. Chem.* **2003**, *11*, 2082–2094.
(20) Kickelbick, G.; Pintauer, T.; Matyjaszewski, K. *New J. Chem.* **2002**, *26*, 462–468.
(21) Pintauer, T.; Matyjaszewski, K. *Coord. Chem. Rev.* **2005**, *249*, 1155–1184 and references cited therein. .
(22) Coullerez, G.; Malmstrom, E.; Jonsson, M. *J. Phys. Chem. A* **2006**, *110*, 10355–10360.
(23) Qiu, J.; Matyjaszewski, K.; Thouin, L.; Amatore, C. *Macromol. Chem. Phys.* **2000**, *201*, 1625–1631.
(24) Braunecker, W. A.; Tsarevsky, N. V.; Gennaro, A.; Matyjaszewski, K. *Macromolecules* **2009**, *42*, 6348–6360.
(25) Nanda, A. K.; Matyjaszewski, K. *Macromolecules* **2003**, *36*, 1487–1493.
(26) Nanda, A. K.; Matyjaszewski, K. *Macromolecules* **2003**, *36*, 599–604.
(27) Di Bernardo, P.; Melchior, P.; Portanova, R.; Tolazzi, M.; Zanonato, P. L. *Coord. Chem. Rev.* **2008**, *252*, 1270–1285.
(28) Di Lena, F.; Matyjaszewski, K. *Dalton Trans.* **2009**, *41*, 8878–8884.
(29) Tsarevsky, N. V.; Braunecker, W. A.; Matyjaszewski, K. *J. Organomet. Chem.* **2007**, *692*, 3212–3222.
(30) Matyjaszewski, K.; Tsarevsky, N. V.; Braunecker, W. A.; Dong, H.; Huang, J.; Jakubowski, W.; Kwak, Y.; Nicolay, R.; Tang, W.; Yoon, J. A. *Macromolecules* **2007**, *40*, 7795–7806.
(31) Nicolay, R.; Kwak, Y.; Matyjaszewski, K. *Angew. Chem., Int. Ed.* **2010**, *49*, 541–544.
(32) Matyjaszewski, K.; Coca, S.; Gaynor, S. G.; Wei, M.; Woodworth, B. E. *Macromolecules* **1997**, *30*, 7348–7350.
(33) Woodworth, B. E.; Metzner, Z.; Matyjaszewski, K. *Macromolecules* **1998**, *31*, 7999–8004.
(34) Percec, V.; Guliashvili, T.; Ladislaw, J. S.; Wistrand, A.; Stjerndahl, A.; Sienkowska, M. J.; Monteiro, M. J.; Sahoo, S. *J. Am. Chem. Soc.* **2006**, *128*, 14156–14165.
(35) Rosen, B. M.; Jiang, X.; Wilson, C. J.; Nguyen, N. H.; Monteiro, M. J.; Percec, V. *J. Polym. Sci., Part A: Polym. Chem.* **2009**, *47*, 5606–5628.
(36) Rosen, B. M.; Percec, B. M. *Chem. Rev.* **2009**, *109*, 5069–5119.
(37) Ahrland, S.; Nilsson, K.; Tagesson, B. *J. Acta Chem. Scand.* **1983**, *37*, 193–201.
(38) Persson, I.; Penner-Hahn, J. E.; Hodgson, K. *Inorg. Chem.* **1993**, *32*, 2497–2501.
(39) Queffelec, J.; Gaynor, S. G.; Matyjaszewski, K. *Macromolecules* **2000**, *33*, 8629–8639.
(40) Gahler, A. R. *Anal. Chem.* **1954**, *26*, 577–579.
(41) Birkin, P. R.; Silva-Martinez, S. *Anal. Chem.* **1997**, *69*, 2055–2062.
(42) Isse, A. A.; Sandonà, G.; Durante, C.; Gennaro, A. *Electrochim. Acta* **2009**, *54*, 3235–3243.
(43) Senne, J. K.; Kratochvil, B. *Anal. Chem.* **1971**, *43*, 79–82.
(44) Di Marco, V. B. Ph.D. Thesis, University of Padova, 1998.
(45) Sillén, L. G. *Acta Chem. Scand.* **1964**, *18*, 1085–1098.
(46) Press,W. H.; Flannery, B. P.; Teukolsky, S. A.; Vetterling, W. T. *Numerical Recipes: The Art of Scientific Computing*; Cambridge University Press: Cambridge, U.K., 1986.
(47) Bard, A. J.; Faulkner, L. R. *Electrochemical Methods*, 2nd ed.; John Wiley & Sons: New York, 2001.
(48) ScQuery v.5.13, The Iupac stability constant database, Academic Software, **2001**.
(49) Heerman, L. F.; Rechnitz, G. A. *Anal. Chem.* **1972**, *44*, 1655–1658.
(50) Manahan, S. E.; Iwamoto, R. T. *Inorg. Chem.* **1965**, *4*, 1409–1413.
(51) Ishiguro, S.; Jeliazkova, B. G.; Ohtaki, H. *Bull. Chem. Soc. Jpn.* **1985**, *58*, 1749–1754.
(52) Kolthoff, I. M.; Coetzee, J. F. *J. Am. Chem. Soc.* **1957**, *79*, 1852.
(53) Del Piero, S.; Fedele, R.; Melchior, A.; Polese, P.; Portanova, R.; Tolazzi, M. *J. Sol. Chem.* **2008**, *37*, 543–551.
(54) Breeze, S. R.; Wang, S. *Inorg. Chem.* **1996**, *35*, 3404–3408.

(55) Tyeklhr, Z.; Jacobson, R. R.; Wei, N.; Murthy, N. N.; Zubieta, J.; Karlin, K. D. *J. Am. Chem. Soc.* **1993**, *115*, 2677–2689.
(56) Thaler, F.; Hubbard, C. D.; Heinemann, F. W.; van Eldik, R.; Schindler, S.; Fábián, I.; Dittler-Klingemann, A. M.; Hahn, F. E.; Orvig, C. *Inorg. Chem.* **1998**, *37*, 4022–4029.
(57) The standard reduction potentials (SRPs) of $Cu^{II}LX$ and $Cu^{II}X_2$ can be calculated from the thermodynamic data reported in tables 1 and 2: (a) $E^{\circ}_{Cu^{II}LX/Cu^{I}LX} = E^{\circ}_{Cu^{II}L/Cu^{I}L} - (RT/F)\ln(K_{Cu^{II}LX}/K_{Cu^{I}LX})$, where $K_{Cu^{I}LX}$ and $K_{Cu^{I}LX}$ are the step stability constants; (b)
$$E^{\ominus}_{Cu^{II}X_2/Cu^{I}X_2} = E^{\ominus}_{Cu^{II}/Cu^{I}} - \frac{RT}{F}\ln(\beta_{Cu^{II}X_2}/\beta_{Cu^{I}X_2})$$
where $\beta_{Cu^{II}X_2}$ and $\beta_{Cu^{I}X_2}$ are the overall stability constants. The SRPs of the binary complexes are about 1 V more positive than those of the ternary complexes.
(58) Tsarevsky, N. V.; Pintauer, T.; Matyjaszewski, K. *Macromolecules* **2004**, *37*, 9768–9778.